Title	Exact Outage Probability of Dual-Hop CSI-Assisted AF Relaying over Nakagami-m Fading Channels
Author(s)	Xia, M; Wu, YC; Aissa, S
Citation	IEEE TRANSACTIONS ON SIGNAL PROCESSING, 2012, v. 60 n. 10, p. 5578-5583
Issued Date	2012
URL	http://hdl.handle.net/10722/189014
Rights	IEEE Transactions on Signal Processing. Copyright © IEEE

Exact Outage Probability of Dual-Hop CSI-Assisted AF Relaying Over Nakagami-m Fading Channels

Minghua Xia, Yik-Chung Wu, and Sonia Aïssa

***Abstract*—In this correspondence, considering dual-hop channel state information (CSI)-assisted amplify-and-forward (AF) relaying over Nakagami-m fading channels, the cumulative distribution function (CDF) of the end-to-end signal-to-noise ratio (SNR) is derived. In particular, when the fading shape factors m_1 and m_2 at consecutive hops take non-integer values, the bivariate H-function and G-function are exploited to obtain an exact analytical expression for the CDF. The obtained CDF is then applied to evaluate the outage performance of the system under study. The analytical results of outage probability coincide exactly with Monte-Carlo simulation results and outperform the previously reported upper bounds in the low and medium SNR regions.**

***Index Terms*—Amplify-and-forward (AF) relaying, channel state information (CSI)-assisted, distribution function, dual-hop, Nakagami-m fading.**

I. Introduction

For dual-hop amplify-and-forward (AF) relaying systems, the gain of relaying node aims to invert the first-hop (source-to-relay) channel and is determined by the channel state information (CSI) of the first hop. According to the amount of CSI obtained at the relay, there are three different AF schemes that can be implemented: blind, semi-blind, and CSI-assisted relaying. Among them, the theoretical analysis of CSI-assisted relaying is extremely important since this scheme characterizes the best performance.

Let γ_1 and γ_2 be the instantaneous signal-to-noise ratios (SNRs) of two consecutive hops, respectively, the end-to-end SNR of CSI-assisted relaying can be derived as $\gamma_{\rm end} = \frac{\gamma_1\gamma_2}{\gamma_1+\gamma_2+1}$[1]. However, due to the existence of the unity in the denominator, which corresponds to the additive white Gaussian noise (AWGN) at the relay, exact performance analysis was usually considered to be intractable over arbitrary Nakagami-m fading channels [1]. For the special case with integer Nakagami-m fading channels, a large number of performance analyses were reported (see [2], [3] and references therein). However, the propagation environments where the Nakagami fading parameter takes non-integer values are very common in practice, such as microcellular scenarios with strong specular components and land mobile satellite channels. Therefore, exact performance analysis of CSI-assisted relaying over arbitrary Nakagami-m fading is of great practical importance, but it still remains an open problem due to potential mathematical difficulty [4].

Manuscript received August 11, 2011; revised February 08, 2012, May 28, 2012, and June 20, 2012; accepted June 20, 2012. Date of publication July 12, 2012; date of current version September 11, 2012. The associate editor coordinating the review of this manuscript and approving it for publication was Dr. Maja Bystrom. The work was supported in part by the Hong Kong University Seed Funding Programme under Project 201111159122, and by King Abdullah University of Science and Technology (KAUST).

M. Xia is with the Division of Computer, Electrical and Mathematical Sciences and Engineering, King Abdullah University of Science and Technology (KAUST), Thuwal 23955-6900, Saudi Arabia (e-mail: minghua.xia@ieee.org).

Y.-C. Wu is with the Department of Electrical and Electronic Engineering, The University of Hong Kong, Hong Kong (e-mail: ycwu@eee.hku.hk).

S. Aïssa is with the Institut National de la Recherche Scientifique (INRS), University of Quebec, Montreal, QC H5A 1K6, Canada (e-mail: aissa@emt.inrs.ca).

Digital Object Identifier 10.1109/TSP.2012.2208104

For the CSI-assisted relaying over arbitrary Nakagami-m fading channels, in order to obtain analytical performance metrics, two upper bounds for $\gamma_{\rm end}$ are widely exploited in the literature. Specifically, the upper bounds are $\gamma_{\rm end} < \frac{\gamma_1\gamma_2}{\gamma_1+\gamma_2}$ and $\gamma_{\rm end} < \min\{\gamma_1, \gamma_2\}$[5]. For the first bound, the AWGN at the relay is ignored and the distribution of $\gamma_{\rm end}$ is replaced by the distribution of the half harmonic mean of γ_1 and γ_2. Based on this approximate distribution for $\gamma_{\rm end}$, a number of analyses have been performed [2], [6]–[10]. For the second bound, it is assumed that γ_1 and γ_2 are non-symmetric and the distribution of $\gamma_{\rm end}$ is replaced by the distribution of the minimum between γ_1 and γ_2. This bound is usually exploited to analyze the average symbol error probability (ASEP) [11], [12], which has the intuitive meaning that the ASEP of the whole link (source-relay-destination) is dominated by the worst link between the source-to-relay and relay-to-destination channels. Recently, the authors of [13] derive the exact probability density function (PDF) of the end-to-end SNR in a single-integral form, considering multi-hop CSI-assisted AF relaying scenario over general Nakagami fading channels.

Although the above bounds seem reasonable at high SNR, they are loose in the low and medium SNR regions. In this paper, the exact cumulative density function (CDF) of the end-to-end SNR of CSI-assisted dual-hop AF relaying is derived in an analytical form, considering transmission over arbitrary Nakagami-m fading channels. In particular, with novel applications of bivariate G-function and H-function, an analytical CDF expression for the case with m taking non-integer values is derived. To the best of the authors' knowledge, this is the first reported exact analytical CDF of the end-to-end SNR in CSI-assisted relaying systems with non-integer Nakagami-m fading parameters, other than the exact single-integral solution in [13]. The obtained CDF is then applied to evaluate outage probability of the system under study. Monte Carlo simulations on outage probability are performed to illustrate the accuracy of our analytical results regardless of the SNR values and, in particular, our analytical results outperform the previously reported upper bounds in the low and medium SNR regions. The novel application of these two special functions are shown to be powerful tools in analyzing the performance of wireless systems in general and relaying techniques in particular.

II. CDF of the End-to-End SNR

For a CSI-assisted dual-hop AF relaying system, the end-to-end SNR from the source to the destination was shown to be exactly given by [1]

$$\gamma_{\rm end} = \frac{\gamma_1\gamma_2}{\gamma_1+\gamma_2+1}, \tag{1}$$

where γ_1 and γ_2 refer to the instantaneous SNRs at the first and second hops, respectively.

Assuming that the channels at two consecutive hops are subject to Nakagami-m fading, the probability density function (PDF) of γ_i in (1), where $i = 1, 2$, is expressed as [14, Eq.(2.21)]

$$f_{\gamma_i}(\gamma_i) = \frac{m_i^{m_i}}{\Gamma(m_i)\bar{\gamma}_i^{m_i}}\gamma_i^{m_i-1}\exp\left(-\frac{m_i}{\bar{\gamma}_i}\gamma_i\right), \quad i = 1, 2 \tag{2}$$

where m_i denotes the Nakagami fading parameter at the $i^{\rm th}$ hop, $\Gamma(\cdot)$ stands for the Gamma function [15, Eq.(8.310)] $\bar{\gamma}_1 \triangleq \mathbb{E}\{|h_{SR}|^2\}\frac{E_S}{\sigma_R^2} = m_1(m_1+1)\frac{E_S}{\sigma_R^2}$, and $\bar{\gamma}_2 \triangleq \mathbb{E}\{|h_{RD}|^2\}\frac{E_S}{\sigma_D^2} =$

$m_2(m_2+1)\frac{E_S}{\sigma_D^2}$ with $\mathbb{E}\{\,.\,\}$ being the statistical expectation operator. Also, the CDF of γ_i is given by [2]

$$F_{\gamma_i}(\gamma_i) = 1 - \frac{1}{\Gamma(m_i)}\Gamma\left(m_i,\, \frac{m_i}{\bar{\gamma}_i}\gamma_i\right), \quad i = 1,\, 2 \tag{3}$$

where $\Gamma(.\,,\,.)$ stands for the upper incomplete Gamma function [15, Eq.(8.350.2)], Finally, by integrating the conditional CDF of γ_{end} with respect to γ_1 over the PDF of γ_1, the CDF of γ_{end} is given by

$$F_{\gamma_{\mathrm{end}}}(\gamma) = 1 - \frac{C_1}{\Gamma(m_2)}\int_0^{\infty}\Gamma\left(m_2,\, \frac{m_2\gamma}{\bar{\gamma}_2}\left(1+\frac{\gamma+1}{x}\right)\right) \times (x+\gamma)^{m_1-1}\exp\left(-\frac{m_1}{\bar{\gamma}_1}(x+\gamma)\right)\mathrm{d}x, \tag{4}$$

where $C_1 \triangleq \frac{m_1^{m_1}}{\left(\Gamma(m_1)\bar{\gamma}_1^{m_1}\right)}$. The integral term in (4) cannot be calculated directly, since the incomplete Gamma function is involved. In order to proceed, two different series expansions of the incomplete Gamma function are exploited and thus two different cases are discussed in the following, depending on the values of the fading parameters m_1 and m_2.

A. Scheme With Integer Values for m_1 and m_2

When m_2 takes integer values, the expansion of the incomplete Gamma function in (4) is a finite series [15, Eq.(8.352.7)], and thus this scheme can be easily analyzed. For the completeness of exposition, the CDF of the end-to-end SNR is reproduced and it is given by [3]

$$F_{\gamma_{\mathrm{end}}}(\gamma) = 1 - 2C_1\sum_{n=0}^{m_2-1}\frac{1}{n!}\left(\frac{m_2}{\bar{\gamma}_2}\right)^n\exp\left[-\left(\frac{m_1}{\bar{\gamma}_1}+\frac{m_2}{\bar{\gamma}_2}\right)\gamma\right] \times \sum_{p=0}^{m_1-1}\sum_{q=0}^{n}\binom{m_1-1}{p}\binom{n}{q}\gamma^{m_1+n-\frac{v_1}{2}} \times (\gamma+1)^{\frac{v_1}{2}}\left(\frac{m_2\bar{\gamma}_1}{m_1\bar{\gamma}_2}\right)^{\frac{v_2}{2}}K_{v_2}\left(2\sqrt{\tilde{\gamma}}\right), \tag{5}$$

where $\binom{n}{k}$ denotes the binomial coefficient, $K_v(x)$ is the v^{th}-order modified Bessel function of the second kind [15, Eq.(8.432.6)], $v_1 \triangleq p+q+1$, $v_2 \triangleq p-q+1$, and $\tilde{\gamma} \triangleq \frac{m_1 m_2\gamma(\gamma+1)}{\bar{\gamma}_1\bar{\gamma}_2}$.

It is known that the Nakagami-m fading reduces to the Rayleigh fading when $m_1 = m_2 = 1$. Accordingly, putting $m_1 = m_2 = 1$ into (5) reduces it to the result previously reported in [16, Eq.(2)].

B. Scheme With Non-Integer Values for m_1 and m_2

When m_2 takes on non-integer values, the expansion of the incomplete Gamma function in (4) is an infinite series [15, Eq.(8.354.2)]. Substituting the infinite series into (4) and performing some algebraic manipulations yield (6) at the bottom of the page.

Although the infinite series representation for the incomplete Gamma function is involved, this series is absolutely convergent for $m_2 \geq 0.5$ and converges rapidly because of the factorial term $n!$ in the denominator. Moreover, the integral term I_1 in (6) can be calculated as [15, Eq.(8.350.2)]

$$I_1 = C_1\left(\frac{\bar{\gamma}_1}{m_1}\right)^{m_1}\int_{\frac{m_1}{\bar{\gamma}_1}\gamma}^{\infty}x^{m_1-1}\exp(-x)\,\mathrm{d}x = \frac{1}{\Gamma(m_1)}\Gamma\left(m_1,\, \frac{m_1}{\bar{\gamma}_1}\gamma\right). \tag{7}$$

For the integral term I_2 in (6), the Newton's generalized binomial theorem $(1+x)^m = \sum_{n=0}^{\infty}\binom{m}{n}x^n$ cannot be applied, since the infinite series on the right-hand side converges only for $|x| < 1$[17, p.28]. Clearly, this condition is not satisfied for the binomials $(1+\frac{\gamma}{x})^{m_1-1}$ and $\left(1+\frac{\gamma+1}{x}\right)^{m_2+n}$ in (6), where $0 < x$ and $\gamma < \infty$. Therefore, how to calculate I_2 becomes challenging, which explains why no analytical CDF for γ_{end} has been reported in the open literature till now. In the sequel, we exploit the Fox's H-function and the generalized Laplace transform of the product of two H-functions to tackle this problem, such that an analytical expression for I_2 is obtained. From the definition of I_2 shown in (6), it can be reformulated as (8) at the bottom of the page, where $\tilde{m}_1 \triangleq \lceil m_1\rceil - m_1$ and $\tilde{m}_2 \triangleq \lceil m_2\rceil - m_2$

$$F_{\gamma_{\mathrm{end}}}(\gamma) = 1 - \underbrace{C_1\int_0^{\infty}(x+\gamma)^{m_1-1}\exp\left(-\frac{m_1}{\bar{\gamma}_1}(x+\gamma)\right)\mathrm{d}x}_{I_1} + \frac{C_1}{\Gamma(m_2)}\sum_{n=0}^{\infty}\frac{(-1)^n}{n!\,(m_2+n)}\left(\frac{m_2}{\bar{\gamma}_2}\gamma\right)^{m_2+n} \times \underbrace{\int_0^{\infty}(x+\gamma)^{m_1-1}\left(1+\frac{\gamma+1}{x}\right)^{m_2+n}\exp\left(-\frac{m_1}{\bar{\gamma}_1}(x+\gamma)\right)\mathrm{d}x}_{I_2}. \tag{6}$$

$$\begin{aligned} I_2 &= \gamma^{m_1-1}(\gamma+1)^{m_2+n}\exp\left(-\frac{m_1}{\bar{\gamma}_1}\gamma\right)\int_0^{\infty}x^{-(m_2+n)}\exp\left(-\frac{m_1}{\bar{\gamma}_1}x\right)\left(1+\frac{x}{\gamma}\right)^{m_1-1}\left(1+\frac{x}{\gamma+1}\right)^{m_2+n}\mathrm{d}x \\ &= \gamma^{m_1-1}(\gamma+1)^{m_2+n}\exp\left(-\frac{m_1}{\bar{\gamma}_1}\gamma\right)\int_0^{\infty}x^{-(m_2+n)}\exp\left(-\frac{m_1}{\bar{\gamma}_1}x\right)\left(1+\frac{x}{\gamma}\right)^{\lceil m_1-1\rceil-\tilde{m}_1}\left(1+\frac{x}{\gamma+1}\right)^{\lceil m_2+n\rceil-\tilde{m}_2}\mathrm{d}x \\ &= \exp\left(-\frac{m_1}{\bar{\gamma}_1}\gamma\right)\sum_{p=0}^{\lceil m_1-1\rceil}\sum_{q=0}^{\lceil m_2+n\rceil}\binom{\lceil m_1-1\rceil}{p}\binom{\lceil m_2+n\rceil}{q}\gamma^{m_1-p-1}(\gamma+1)^{m_2+n-q} \\ &\quad\times\int_0^{\infty}x^{p+q-(m_2+n)}\exp\left(-\frac{m_1}{\bar{\gamma}_1}x\right)\left(1+\frac{x}{\gamma}\right)^{-\tilde{m}_1}\left(1+\frac{x}{\gamma+1}\right)^{-\tilde{m}_2}\mathrm{d}x, \end{aligned} \tag{8}$$

with $\lceil . \rceil$ being the integer ceiling operator, and the binomial expansion was exploited to reach (8). Applying the equality $(1+x)^{-\alpha} = \frac{1}{\Gamma(\alpha)} H_{1,\,1}^{1,\,1}\left[x \left| \begin{matrix} (1-\alpha,\,1) \\ (0,\,1) \end{matrix} \right. \right]$ with $\alpha \geq 0$[18, p.152] to (8), where $H[\,x\,|\,.\,]$ is the Fox's H-function [18], we can express I_2 as (9) at the bottom of the page. Then, using the generalized Laplace transform of the product of two H-functions[1][18, Eq.(2.6.2)], we obtain (10)–(11) at the bottom of the page, where [20, Eq.(6.4.1)] was exploited to arrive at (11) with H_1 denoting the bivariate H-function and G_1 being the bivariate G-function [19], which are given by

$$\mathrm{H}_1 \triangleq H^{1,\,1,\,1,\,1,\,1}_{1,\,[1:\,1],\,0,\,[1:\,1]} \left[\begin{matrix} \frac{\tilde{\gamma}_1}{m_1\gamma} \\ \frac{\tilde{\gamma}_1}{m_1(\gamma+1)} \end{matrix} \left| \begin{matrix} (1+p+q-m_2-n,\,1) \\ (1-\tilde{m}_1,\,1);\,(1-\tilde{m}_2,\,1) \\ - \\ (0,\,1);\,(0,\,1) \end{matrix} \right. \right] \quad (12)$$

and

$$\mathrm{G}_1 \triangleq G^{1,\,1,\,1,\,1,\,1}_{1,\,[1:\,1],\,0,\,[1:\,1]} \left[\begin{matrix} \frac{\tilde{\gamma}_1}{m_1\gamma} \\ \frac{\tilde{\gamma}_1}{m_1(\gamma+1)} \end{matrix} \left| \begin{matrix} 1+p+q-m_2-n \\ 1-\tilde{m}_1;\,1-\tilde{m}_2 \\ - \\ 0;\,0 \end{matrix} \right. \right], \quad (13)$$

respectively.

Finally, substituting (7), (11), and C_1 into (6) and performing some algebraic manipulations, we obtain the CDF of the end-to-end SNR of dual-hop CSI-assisted relaying systems as (14) at the bottom of the page, where $C_2 \triangleq \frac{1}{(\Gamma(m_1)\,\Gamma(m_2)\,\Gamma(\tilde{m}_1)\,\Gamma(\tilde{m}_2))}$.

The infinite series in (14) is absolutely convergent. This is demonstrated as follows. Firstly, the bivariate G-function $G^{n,\,v_1,\,v_2,\,w_1,\,w_2}_{p,\,[t_1:\,t_2],\,s,\,[q_1:\,q_2]} \left[\begin{smallmatrix} x \\ y \end{smallmatrix} \middle| . \right]$ is defined in terms of double Mellin-Barnes type integrals, and it converges if the following conditions are satisfied [21, p.62]:

$$p + q_1 + s + t_1 < 2(n + v_1 + w_1), \quad (15)$$

$$p + q_2 + s + t_2 < 2(n + v_2 + w_2), \quad (16)$$

$$|\arg(x)| < \pi \left[n + v_1 + w_1 - \frac{(p + q_1 + s + t_1)}{2} \right], \quad (17)$$

$$|\arg(y)| < \pi \left[n + v_2 + w_2 - \frac{(p + q_2 + s + t_2)}{2} \right]. \quad (18)$$

It is easy to show that the parameters of the G-function in (13) satisfy these sufficient conditions above and, therefore, the G-function converges in the sense of finite value. Secondly, it is clear that the infinite series in (14) is an alternating series and thus, by use of the Leibnitz's test [17, Theorem 1.5], it is known that this infinite series is conditionally convergent because of the factorial term $n!$ in the denominator of the summand. Furthermore, applying the ratio test to the associated series of positive terms yields the infinite series in (14) to be absolutely convergent.

Note that the bivariate G-function cannot be directly computed by popular mathematical softwares such as Matlab and Mathematica. In general, it has to be computed by its definition in terms of the double Mellin-Barnes type integrals [19], such as the Mathematica algorithm recently developed in [22]. Unfortunately, this definition is non-analytical and computationally intensive. In the following, we develop a general analytical expression to compute the bivariate G-function in the form of (13), which can also be applied to address other theoretical problems.

Since the convergence of the bivariate G-function in the form of (13) is guaranteed as per (15)–(18), according to [19, Eq.(2.3)], it can be expanded as (19)–(20) at the bottom of the next page, where in (19) the symbol $(a)_b = \frac{\Gamma(a+b)}{\Gamma(a)}$ denotes the Pochhammer operator, and we used

[1]There are several conditions need to be satisfied. They were carefully checked but omitted here due to space limitation.

$$I_2 = \exp\left(-\frac{m_1}{\bar{\gamma}_1}\gamma\right) \sum_{p=0}^{\lceil m_1-1\rceil} \sum_{q=0}^{\lceil m_2+n\rceil} \binom{\lceil m_1-1\rceil}{p} \binom{\lceil m_2+n\rceil}{q} \gamma^{m_1-p-1} (\gamma+1)^{m_2+n-q} \times \frac{1}{\Gamma(\tilde{m}_1)\Gamma(\tilde{m}_2)} \int_0^\infty x^{p+q-(m_2+n)} \exp\left(-\frac{m_1}{\bar{\gamma}_1}x\right) H_{1,\,1}^{1,\,1}\left[\frac{x}{\gamma}\,|\,(1-\tilde{m}_1,\,1)(0,\,1)\right] H_{1,\,1}^{1,\,1}\left[\frac{x}{\gamma+1}\,\middle|\,\begin{matrix}(1-\tilde{m}_2,\,1)\\(0,\,1)\end{matrix}\right] \mathrm{d}x. \quad (9)$$

$$I_2 = \frac{\exp\left(-\frac{m_1}{\bar{\gamma}_1}\gamma\right)}{\Gamma(\tilde{m}_1)\Gamma(\tilde{m}_2)} \sum_{p=0}^{\lceil m_1-1\rceil} \sum_{q=0}^{\lceil m_2+n\rceil} \binom{\lceil m_1-1\rceil}{p} \binom{\lceil m_2+n\rceil}{q} \gamma^{m_1-p-1} (\gamma+1)^{m_2+n-q} \left(\frac{m_1}{\bar{\gamma}_1}\right)^{m_2+n-p-q-1} \mathrm{H}_1 \quad (10)$$

$$= \frac{\exp\left(-\frac{m_1}{\bar{\gamma}_1}\gamma\right)}{\Gamma(\tilde{m}_1)\Gamma(\tilde{m}_2)} \sum_{p=0}^{\lceil m_1-1\rceil} \sum_{q=0}^{\lceil m_2+n\rceil} \binom{\lceil m_1-1\rceil}{p} \binom{\lceil m_2+n\rceil}{q} \gamma^{m_1-p-1} (\gamma+1)^{m_2+n-q} \left(\frac{m_1}{\bar{\gamma}_1}\right)^{m_2+n-p-q-1} \mathrm{G}_1, \quad (11)$$

$$F_{\gamma_{\mathrm{end}}}(\gamma) = 1 - \frac{1}{\Gamma(m_1)}\Gamma\left(m_1,\,\frac{m_1}{\bar{\gamma}_1}\gamma\right) + C_2 \exp\left(-\frac{m_1}{\bar{\gamma}_1}\gamma\right) \sum_{n=0}^{\infty} \frac{(-1)^n}{n!\,(m_2+n)} \left(\frac{m_2}{\bar{\gamma}_2}\gamma\right)^{m_2+n} \times \sum_{p=0}^{\lceil m_1-1\rceil} \sum_{q=0}^{\lceil m_2+n\rceil} \binom{\lceil m_1-1\rceil}{p} \binom{\lceil m_2+n\rceil}{q} \left(\frac{m_1}{\bar{\gamma}_1}\gamma\right)^{m_1-p-1} \left(\frac{m_1}{\bar{\gamma}_1}(\gamma+1)\right)^{m_2+n-q} \mathrm{G}_1, \quad (14)$$

the symbolic operators proposed in [23] to derive (20), which is a single series of the product of two generalized hypergeometric functions [15, Eq.(9.14.1)]. Note that the parameters a, $1-b_1$, and $1-b_2$ cannot take negative integers since Gamma function is involved in (19)–(20), which is satisfied when non-integer m_1 and m_2 are applied to (13). Although it seems complicated, (20) involves only common special functions and it can be easily evaluated in a numerical way. The accuracy of (20) is corroborated by simulation results in the next section.

Remark II.1. (The PDF of the End-to-End SNR): After obtaining the CDF of the end-to-end SNR of CSI-assisted relaying over arbitrary Nakagami-m fading channels, its corresponding PDF can be readily obtained by taking the derivative of $F_{\gamma_{\rm end}}(\gamma)$ with respect to γ. More specifically, the derivative of $K_v(\gamma)$ in (5) with respect to γ can be obtained by using [15, Eq.(8.486.12)]. On the other hand, as a special case of bivariate H-function [20, Eq.(6.4.1)], the derivative of G_1 in (14) can be obtained by exploiting the derivative of bivariate H-function shown in [20, Eq.(6.5.7)].

III. Outage Probability

Once the CDF and PDF of the end-to-end SNR have been obtained, they can be widely applied to evaluate the system performance in terms of different performance metrics. Based on the CDF, for example, the outage probability, outage capacity, and codeword error probability can be analytically obtained. On the other hand, by exploiting the PDF, the ergodic capacity and the output statistics such as the moments of the output SNR can be numerically evaluated. Herein, due to page limitation, we only demonstrate the accuracy of our main result (14) using outage probability. In all simulations, without loss of generality, the variances of the AWGN at the relay and at the destination are assumed to be identical, that is, $\sigma_R^2 = \sigma_D^2$. Furthermore, the values of (14) are computed with the first 9 terms of the infinite series, in which the function G_1 is also computed with its first 9 terms as per (20). Further test results show that, when more than 9 terms from the infinite series in (20) are involved, both the proposed method and that in [22] yield almost the same output.

Outage probability, $P(\gamma_{\rm th})$, is defined as the probability that the instantaneous output SNR falls below a pre-defined threshold $\gamma_{\rm th}$. Hence, evaluating the CDF (5) or (14) at $\gamma_{\rm th}$, we obtain

$$P(\gamma_{\rm th}) = \Pr\{\gamma_{\rm end} < \gamma_{\rm th}\} = F_{\gamma_{\rm end}}(\gamma_{\rm th}). \tag{21}$$

For comparison purposes, the outage probability based on the two upper bounds discussed in Section I are also reproduced here. For the first bound $\gamma_{\rm end} < \frac{\gamma_1\gamma_2}{\gamma_1+\gamma_2}$ with the symmetric fading shape factors $m_1 = m_2 = m$, the outage probability is given by [6, Eq.(18)]

$$P^{\rm b1}(\gamma_{\rm th}) = \frac{\sqrt{\pi}}{2^{2m-3}\,\Gamma^2(m)}\left(\frac{m}{\bar{\gamma}}\gamma_{\rm th}\right) \times G_{2,3}^{2,1}\left[\frac{4\,m}{\bar{\gamma}}\gamma_{\rm th}\,\middle|\,\begin{matrix}(0,\,m-0.5)\\(m-1,\,2m-1,\,-1)\end{matrix}\right] \tag{22}$$

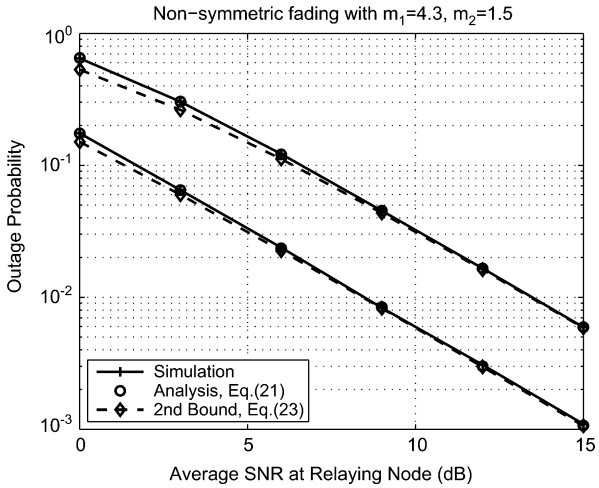

Fig. 1. Outage probability of dual-hop CSI-assisted AF relaying systems with non-symmetric non-integer Nakagami-m fading parameters.

where the superscript b_1 of $P^{\rm b1}(\gamma_{\rm th})$ refers to the first bound, and $G[\,.\,|\,.\,]$ denotes the Meijer's G-function [15, Eq.(9.301)]. For the non-symmetric case with non-integer values $m_1 \neq m_2$, to the best of our knowledge, no result was ever reported.

For the second bound $\gamma_{\rm end} < \min\{\gamma_1,\,\gamma_2\}$, the outage probability is clearly given by

$$P^{\rm b2}(\gamma_{\rm th}) = F_{\gamma_1}(\gamma_{\rm th}) + F_{\gamma_2}(\gamma_{\rm th}) - F_{\gamma_1}(\gamma_{\rm th})F_{\gamma_2}(\gamma_{\rm th}), \tag{23}$$

where the superscript b_2 of $P^{\rm b2}(\gamma_{\rm th})$ refers to the second bound.

Fig. 1 shows the outage probability of the systems with non-symmetric non-integer fading parameters $(m_1,\,m_2) = (4.3,\,1.5)$, and the threshold $\gamma_{\rm th} = 0,\,5$ dB. It is observed that the analytical results based on (21) coincide perfectly with the simulation results whereas the second bound (23) yields a small gap at low SNR. Notice that, since the first bound (22) holds only in the symmetric fading case (i.e., the fading parameters $m_1 = m_2 = m$), it cannot be applied to this non-symmetric fading scenario $(m_1 \neq m_2)$.

Fig. 2 presents the outage probability with symmetric non-integer fading parameters $m_1 = m_2 = 1.5$, and the threshold $\gamma_{\rm th} = 0,\,5$ dB. It is observed that the bound (23) performs worst and it is very loose in the whole SNR region under consideration, since this bound is derived with the assumption that the SNRs at consecutive hops are non-symmetric. The first bound (22) performs a little better than the second bound (23) but it is still loose in the low SNR region, since the effect of AWGN is ignored. On the other hand, our analytical result in (21) is always consistent with the simulation results.

$$G_{1,[1:1],0,[1:1]}^{1,1,1,1,1}\left[\begin{matrix}x\\y\end{matrix}\,\middle|\,\begin{matrix}a\\b_1;\ b_2\\-\\0;\ 0\end{matrix}\right] = \Gamma(a)\,\Gamma(1-b_1)\,\Gamma(1-b_2)\sum_{p=0}^{\infty}\sum_{q=0}^{\infty}\frac{1}{p!\,q!}(a)_{p+q}(1-b_1)_p\,(1-b_2)_q\,(-x)^p\,(-y)^q \tag{19}$$

$$= \Gamma(a)\,\Gamma(1-b_1)\,\Gamma(1-b_2)\sum_{r=0}^{\infty}\frac{1}{r!}(a)_r\,(1-b_1)_r\,(1-b_2)_r \times x^r y^r\ {}_2F_0\,(a+r,\,1-b_1+r;-;-x)\ {}_2F_0\,(a+r,\,1-b_2+r;-;-y)\,, \tag{20}$$

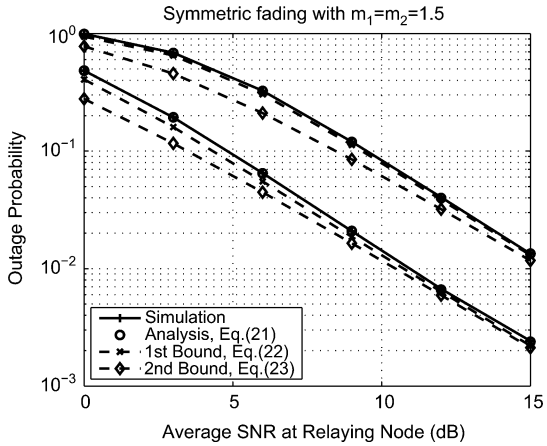

Fig. 2. Outage probability of dual-hop CSI-assisted AF relaying systems with symmetric non-integer Nakagami-m fading parameters.

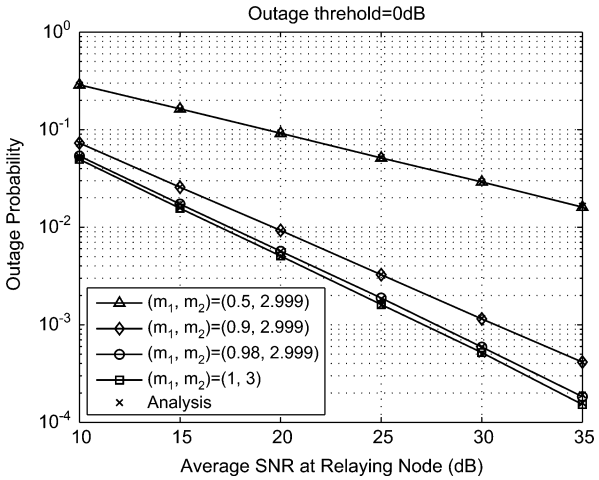

Fig. 3. Outage probability of dual-hop CSI-assisted AF relaying systems (non-integer versus integer fading parameters).

Note that the CDF expression of the non-integer case in (14) cannot reduce to that of the integer case in (5). This is because we exploited two exclusive series expansions of the incomplete Gamma functions $\Gamma(m,\ x)$ with respect to the integer and non-integer values of m [15, Eqs.(8.352.7) & (8.354.2)], respectively. However, when a non-integer value of m closely approaches an integer value, these two expansions should have almost the same numerical value; in other words, the result of (14) should be almost the same as that of (5). This is illustrated in Fig. 3. This figure shows the outage probability of different non-integer fading scenarios, compared with the integer fading scenario where $(m_1,\ m_2) = (1,\ 3)$. For the non-integer cases, the fading parameter m_2 at the second hop is set to $m_2 = 2.999$, which is almost identical to the integer case with $m_2 = 3$. On the other hand, the fading parameter m_1 at the first hop varies from the worst case $m_1 = 0.5$ to $m_1 = 0.9$ and finally $m_1 = 0.98$. It is observed that, the worst fading parameter $m_1 = 0.5$ results in the highest outage probability. When m_1 increases, the outage probability of non-integer cases decreases and it becomes closer and closer to that of the integer case. Also, the analytical results coincide perfectly with the simulation results. This demonstrates the effectiveness of our derivations.

Finally, comparing Fig. 1 with Fig. 2, we observe that the slopes of all curves are identical at high SNR. Moreover, the slopes of the curves in Fig. 3 improve with m_1. These observations are in agreement with the well-known result that the diversity order of dual-hop AF relaying systems is given by $\min\{m_1,\ m_2\}$[4], [24].

IV. Conclusion

Due to the difficulty of mathematical derivation, analyzing the performance of CSI-assisted AF relaying transmission in an exact way is very challenging, especially when the transmission is performed over the general Nakagami-m fading channels. In this paper, exact expression for the distribution function of the end-to-end SNR was derived. In particular, when m takes non-integer values, the Fox's H-function, bivariate H-function and G-function were exploited. Simulation results of outage probability corroborated all analytical results and these special functions were shown to be efficient tools for system performance evaluation.

References

[1] M. O. Hasna and M.-S. Alouini, "End-to-end performance of transmission systems with relays over Rayleigh-fading channels," *IEEE Trans. Wireless Commun.*, vol. 2, no. 6, pp. 1126–1131, Nov. 2003.

[2] D. B. da Costa and S. Aïssa, "Cooperative dual-hop relaying systems with beamforming over Nakagami-m fading channels," *IEEE Trans. Wireless Commun.*, vol. 8, no. 8, pp. 3950–3954, Aug. 2009.

[3] D. Senaratne and C. Tellambura, "Unified exact performance analysis of two-hop amplify-and-forward relaying in Nakagami fading," *IEEE Trans. Veh. Technol.*, vol. 59, no. 3, pp. 1529–1534, Mar. 2010.

[4] M. Xia, C. Xing, Y.-C. Wu, and S. Aïssa, "Exact performance analysis of dual-hop semi-blind AF relaying over arbitrary Nakagami-m fading channels," *IEEE Trans. Wireless. Commun.*, vol. 10, no. 10, pp. 3449–3459, Oct. 2011.

[5] A. Bletsas, A. Khisti, D. P. Reed, and A. Lippman, "A simple cooperative diversity method based on network path selection," *IEEE J. Sel. Areas Commun.*, vol. 24, no. 3, pp. 659–672, Mar. 2006.

[6] M. O. Hasna and M.-S. Alouini, "Harmonic mean and end-to-end performance of transmission systems with relays," *IEEE Trans. Commun.*, vol. 52, no. 1, pp. 130–135, Jan. 2004.

[7] L.-L. Yang and H.-H. Chen, "Error probability of digital communications using relay diversity over Nakagami-m fading channels," *IEEE Trans. Wireless Commun.*, vol. 7, no. 5, pp. 1806–1811, May 2008.

[8] N. C. Beaulieu and Y. Chen, "An accurate approximation to the average error probability of cooperative diversity in Nakagami-m fading," *IEEE Trans. Wireless Commun.*, vol. 9, no. 9, pp. 2707–2711, Sep. 2010.

[9] V. Asghari, A. Maaref, and S. Aïssa, "Symbol error probability analysis for multihop relaying over Nakagami fading channels," in *Proc. IEEE Wireless Commun. Networking Conf. (WCNC)*, Sydney, Australia, Apr. 2010, pp. 1–5.

[10] M. Xia and S. Aïssa, "Moments based framework for performance analysis of one-way/two-way CSI-assisted AF relaying," *IEEE J. Sel. Areas Commun.*, vol. 30, no. 8, Sep. 2012.

[11] D. B. da Costa and S. Aïssa, "End-to-end performance of dual-hop semi-blind relaying systems with partial relay selection," *IEEE Trans. Wireless Commun.*, vol. 8, no. 8, pp. 4306–4315, Aug. 2009.

[12] S. Ikki and S. Aïssa, "Performance analysis of dual-hop relaying systems in the presence of co-channel interference," in *Proc. IEEE Global Commun. Conf. (IEEE Globecom)*, Miami, FL, Dec. 2010, pp. 1–5.

[13] N. C. Beaulieu and S. S. Soliman, "Exact analytical solution for end-to-end SNR of multihop AF relaying systems," in *Proc. IEEE Workshop Mobile Comput. Emerging Commun. Netw. (IEEE Globecom)*, Houston, TX, Dec. 2011, pp. 580–585.

[14] M. K. Simon and M.-S Alouini, *Digital Communication Over Fading Channels*, 2nd ed. New York: Wiley, 2005.

[15] I. S. Gradshteyn and I. M. Ryzhik, *Table of Integrals, Series, and Products*, 7th ed. New York: Academic, 2007.

[16] B. Barua, H. Q. Ngo, and H. Shin, "On the SEP of cooperative diversity with opportunistic relaying," *IEEE Commun. Lett.*, vol. 12, no. 10, pp. 727–729, Oct. 2008.

[17] L. C. Andrews, *Special Functions of Mathematics for Engineers*, 2nd ed. New York: McGraw-Hill, 1992.

[18] A. M. Mathai and R. K. Saxena, *The H-Function With Applications in Statistics and Other Disciplines*. New Delhi, India: Wiley Eastern, 1978.

[19] R. P. Agarwal, "An extension of Meijer's G-function," *Proc. Nat. Inst. Sci. India, Part A*, vol. 31, pp. 536–546, 1965.

[20] H. M. Srivastava, K. C. Gupta, and S. P. Goyal, *The H-Functions of One and Two Variables With Applications*. New Delhi, India: South Asian Publishers, 1982.
[21] A. M. Mathai and R. K. Saxena, "Expansion of Meijer's G-function of two variables when the upper parameters differ by integers," *Kyungpook Math. J.*, vol. 12, no. 1, pp. 61–68, Jun. 1972.
[22] I. S. Ansari, S. Al-Ahmadi, F. Yilmaz, M.-S. Alouini, and H. Yanikomeroglu, "A new formula for the BER of binary modulations with dual-brance selection over gereralized-K composite fading channels," *IEEE Trans. Commun.*, vol. 59, no. 10, pp. 2654–2658, Oct. 2011.
[23] J. L. Burchnall and T. W. Chaundy, "Expansion of Appell's double hypergeometric functions," *Quart. J. Math. (Oxford)*, vol. 11, pp. 249–270, Nov. 1940.
[24] Y. Li and S. Kishore, "Asymptotic analysis of amplify-and-forward relaying in Nakagami-fading environments," *IEEE Trans. Wireless Commun.*, vol. 6, no. 12, pp. 4256–4262, Nov. 2007.

Optimal Phase Response Functions for Fast Pulse-Coupled Synchronization in Wireless Sensor Networks

Yongqiang Wang and Francis J. Doyle, III

***Abstract*—Synchronization is crucial to wireless sensor networks. Recently, a pulse-coupled synchronization strategy that emulates biological pulse-coupled agents has been used to achieve this goal. We propose to optimize the phase response function such that synchronization rate is maximized. Since the synchronization rate is increased independently of transmission power, energy consumption is reduced, hence extending the life of battery-powered sensor networks. A comparison with existing phase response functions confirms the effectiveness of the method.**

***Index Terms*—Phase response function, pulse-coupled oscillators, synchronization rate, wireless sensor networks.**

I. Introduction

Pulse-coupled oscillators (PCOs) have received increased attention in past decades. It is an effective tool to describe many biological synchronization phenomena such as the flashing of fireflies, the contraction of cardiac cells and the firing of neurons [1], [2]. Due to its importance in biological oscillations, PCOs have been extensively studied in the life science literature [3].

Recently, the PCO based synchronization strategy has been applied to wireless sensor networks. In pulse-coupled synchronization strategy, each sensor marks its individual time slot starting point by sending a pulse, and by adjusting its state upon receiving a pulse from adjacent nodes, the whole network can be synchronized [4]–[6]. Since PCOs can be synchronized via pulse transmitting instead of packet exchanging, it avoids wasting the limited computational capability of sensor nodes which is required by packet based synchronization algorithms. Moreover, the pulse-coupled synchronization strategy does not require any memory to store the information of neighboring nodes, which is of great appeal to low cost sensor nodes. Therefore, the PCO based synchronization scheme has received increased attention in the communication community recently. For example, the authors in [5] discussed the implementation of PCOs in a wide band network, the authors in [7] verified the effectiveness of PCO based synchronization strategy using a TinyOS simulator. The authors in [8] and [9] discussed the scalability of pulse-coupled strategy when used to synchronize sensor networks. The authors in [10] and [11] gave the maximal allowable refractory period of PCOs when applied to synchronize wireless sensor networks.

In PCOs, oscillators interact in a pulsatile rather than a smooth manner. This effect can be captured as a phase response function [12]. The phase response function tabulates the shift in the phase of an oscillation induced by a perturbation as a function of the phase at which the perturbation is received. It has been proven to play an important role in the synchronization process [3], [12]–[16]. However, in published applications of pulse-coupled strategies to wireless sensor network synchronization, the phase response function is not strategically designed. We propose to optimize the phase response function such that the synchronization rate is maximized. Given that energy consumption in the synchronization process is determined by the product of transmission power and time to synchronization, which correspond to coupling strength and synchronization rate, respectively, our optimal phase response function saves the energy consumed in the synchronization process since it is independent of coupling strength. This has great significance in wireless sensor networks, where sensors are typically battery driven.

II. Problem Formulation and Model Transformation

Consider N pulse-coupled oscillators $\dot{x}_i = f_i(x_i)$ where f_i is the dynamics and $x_i \in [0,1]$ is the state ($i = 1,2\ldots,N$). When x_i reaches 1, oscillator i fires (emits a pulse) and resets x_i to 0. When oscillator i receives a pulse from an adjacent oscillator (e.g., oscillator j), it shifts x_i to $x_i + l$ or 1, whichever is less, i.e., [2]

$$x_j(t) = 1 \Longrightarrow x_i(t^+) = \min\{1, x_i(t) + l\}, \quad l \in (0,1] \tag{1}$$

The shift in state can be modeled by a Dirac function $\delta(t)$, which is zero for all values of t except $t = 0$ and satisfies $\int_{-\infty}^{\infty} \delta(t)dt = 1$. The coupled dynamics is given by [12]:

$$\dot{x}_i = f_i(x_i) + \sum_{1 \le j \le N, j \ne i} l a_{i,j} \delta(t - t_j), \quad i = 1,2,\ldots,N \tag{2}$$

where $a_{ij} \in \{0,1\}$ denotes the effect of oscillator j on oscillator i: when x_j reaches 1 (at t_j), oscillator j fires and resets x_j to 0, and at the same time pulls oscillator i up by an amount $la_{i,j}$.

Remark 1: If $a_{i,j}$ is 0, then oscillator i is not affected by oscillator j.

Assumption 1: We assume that the interaction is bidirectional, i.e., $a_{i,j} = a_{j,i}$, which is common in wireless networks [17]. We also assume that the interaction topology is connected, i.e., there is a multi-hop path (i.e., a sequence with nonzero values a_{i,m_1}, $a_{m_1,m_2},\ldots,a_{m_{p-1},m_p}, a_{m_p,j}$) from each node i to every other node j.

Assumption 2: We assume that the coupling is weak, i.e., $l \ll 1$ [15].

Manuscript received May 05, 2012; accepted June 27, 2012. Date of publication July 11, 2012; date of current version September 11, 2012. The associate editor coordinating the review of this manuscript and approving it for publication was Prof. YaoWin (Peter) Hong. The work was supported in part by the U.S. Army Research Office through Grant W911NF-07-1-0279, National Institutes of Health through Grant GM078993, and the Institute for Collaborative Biotechnologies through grant W911NF-09-0001 from the U.S. Army Research Office. The content of the information does not necessarily reflect the position or the policy of the Government, and no official endorsement should be inferred.

The authors are with the Institute for Collaborative Biotechnologies, University of California, Santa Barbara, CA 93106-5080 USA (e-mail: wyqthu@gmail.com; frank.doyle@icb.ucsb.edu).

Color versions of one or more of the figures in this paper are available online at http://ieeexplore.ieee.org.

Digital Object Identifier 10.1109/TSP.2012.2208109